JCEC
THE JOURNAL OF ENGINEERING AND EXACT SCIENCES

OPEN ACCESS

The Journal of Engineering and Exact Sciences – jCEC, Vol. 10 N. 05 (2024)
journal homepage: https://periodicos.ufv.br/jcec
eISSN: 2527-1075
ISSN: 2446-9416

Development of a pressure acquisition system for detecting mandibular movements in ruminants

Desenvolvimento de um sistema para aquisição de pressão para detecção de movimentos mandibulares em ruminantes

Article Info:
Article history: Received 2024-05-04 / Accepted 2024-06-20 / Available online 2024-06-25
doi: 10.18540/jcecvl10iss5pp19060

Geraldo Loyola Baiôco
ORCID: https://orcid.org/0009-0001-6406-4746
Universidade Tecnológica Federal do Paraná - Campus Pato Branco, Brazil
E-mail: baiocogeraldo@gmail.com
Fábio Luiz Bertotti
ORCID: https://orcid.org/0000-0002-9402-0824
Universidade Tecnológica Federal do Paraná - Campus Pato Branco, Brazil
E-mail: bertotti@utfpr.edu.br
André Luis Finkler da Silveira
ORCID: https://orcid.org/0000-0001-6071-5444
Instituto de Desenvolvimento Rural do Paraná - IDR-PR, Brazil
E-mail: andrefinkler@idr.pr.gov.br
João Ari Gualberto Hill
ORCID: https://orcid.org/0000-0003-4175-6042
Instituto de Desenvolvimento Rural do Paraná - IDR-PR, Brazil
E-mail: joaohill@idr.pr.gov.br

Resumo
A Pecuária é responsável pela produção de grande parte da proteína animal consumida pelos seres humanos. As estimativas de um crescimento significativo da população mundial ao longo anos evidenciam uma demanda não apenas na expansão da produção animal, mas também um aumento da eficiência na pecuária. Para isso, um dos fatores importantes consiste no aprimoramento do processo de nutrição, sendo fundamental a análise do comportamento ingestivo de ruminantes. Diante disso, este trabalho apresenta o desenvolvimento de um sistema para aquisição, armazenamento e transmissão de sinais de um sensor de pressão para o monitoramento e a avaliação dos movimentos mastigatórios em ruminantes. Nesse sistema foi utilizado um sensor de pressão para obter sinais referentes ao movimento mastigatório. Esses sinais são adquiridos por um microcontrolador a uma frequência de 100 Hz, transmitidos para um smartphone via comunicação bluetooth e armazenados em um cartão de memória para posterior análise. Testes preliminares em bancada foram realizados com o sistema instalado em uma cabeça de bovino prototipada em tamanho real. Movimentos de compressão foram aplicados em um tubo de silicone, provocando variações de pressão no sensor. A partir da transmissão dos dados a um smartphone via comunicação bluetooth foi possível verificar o sinal e ajustar o ganho do amplificador de instrumentação e realizar o melhor posicionamento do tubo de silicone no buçal. Com a leitura dos dados gravados em cartão de memória foi possível obter o perfil do sinal, demonstrando-se de forma gráfica que o sinal corresponde ao perfil típico para esse tipo de sensor.
Palavras-chave: Sensor de pressão. Aquisição de sinais. Microcontrolador. Pecuária de precisão. Comportamento ingestivo.

Abstract
Livestock farming is responsible for producing much of the animal protein that humans consume. Estimates of significant growth in the world population over the years highlight a demand not only for the expansion of animal production but also for an increase in livestock efficiency. To achieve this, one of the essential factors is improving the nutrition process, with the analysis of the ingestive behavior of ruminants being essential. Therefore, this work presents the development of a system for acquiring, storing, and transmitting signals from a pressure sensor for monitoring and evaluating masticatory movements in ruminants. This system employs a pressure sensor to obtain signals relating to chewing movement. A microcontroller acquires these signals at a sampling frequency of 100 Hz, and the resulting data are transmitted to a smartphone via Bluetooth and stored in a memory card for later analysis. Preliminary bench tests were carried out with the system installed on a full-size prototyped bovine head. Compression movements were applied to a silicone tube, causing pressure variations in the sensor. By transmitting the data to a smartphone via Bluetooth, it was possible to check the signal, adjust the gain of the instrumentation amplifier, and achieve the best positioning of the silicone tube in the mouthpiece. By reading the data recorded on a memory card, it was possible to obtain the signal profile, graphically demonstrating that the signal corresponds to the typical profile for this type of sensor.
Keywords: Pressure sensor. Signal acquisition. Microcontrolller. Precision farming. Ingestive behavior.

1. Introduction

According to the United Nations, the estimated world population in 2022 was 8 billion people, while projections for 2030, 2050, and 2100 are 8.5, 9.7, and 10.4 billion people, respectively (United Nations, 2022). With this population increase, animal protein consumption is expected to increase by 14% by 2030, compared to the average for the base period from 2018 to 2020. This growth intensifies the environmental impacts caused by livestock farming and threatens access to food for the poorest population (OECD/FAO, 2021). These projections show that solutions are needed to anticipate problems arising from the intensification of animal production, increase productivity, and reduce the environmental impacts of the process.

The increase in livestock efficiency must be achieved by implementing the concept of Precision Livestock Farming (PLF), which, in general terms, consists of measuring variables in animals, modeling the data to select relevant information, and using these models in real-time for the monitoring and control, seeking to achieve a result closer to the animal's genetic potential (Berckmans, 2008; Berckmans, 2017). Compared to other industry sectors, livestock farming is underdeveloped in monitoring and controlling production, and this is because the variables to be monitored are naturally unpredictable (Schofield et al., 2002). Therefore, tools are needed so that precision livestock farming can achieve its objective of providing information on animal health, welfare, and productivity more frequently and in detail so that the producer can make quick and assertive management decisions (Norton et al., 2018).

Among the various parameters that can be obtained from animals, those associated with ingestion stand out, as changes in the animal's ingestive behavior can indicate health problems in dairy cattle (Ribas et al., 2017). There are several manual and automatic methods for monitoring animal ingestive behavior. The visual method is based on the observation, identification, and counting of the animal's chewing movements, and despite being considered the reference method, it is laborious and impracticable for many animals. Automatic methods rely on various biosensors, which quantify animals' behavioral, physiological, and immunological responses. A range of biosensors are used to identify mandibular movements, such as mechanical and acoustic sensors, accelerometers, and electromyographs (Neethirajan et al., 2017).

In the category of mechanical sensors, initially, there were pneumographs (Law & Sudweeks, 1975), evolving into tubes of carbon granules with variable electrical resistance due to deformation (Penning, 1983), similar to strain gauges (Beauchemin et al., 1989). The reference systems for the

primary research carried out in the area are: 1- IGER behavior recorder (from the Institute of Grassland and Environmental Research) with correlations in the range of 91% and 95% for chewing and rumination movements compared with the visual method in a 5-minute window (Rutter et al., 1997); and the ART-MSR (Agroscope Reckenholz-Tänikon Research Institute, Modular Signal Recorder) pressure sensor (Nydegger et al., 2011). For IGER, the Graze computer program was developed to visualize the obtained signal (Rutter et al., 2000), as illustrated in Figure 1.

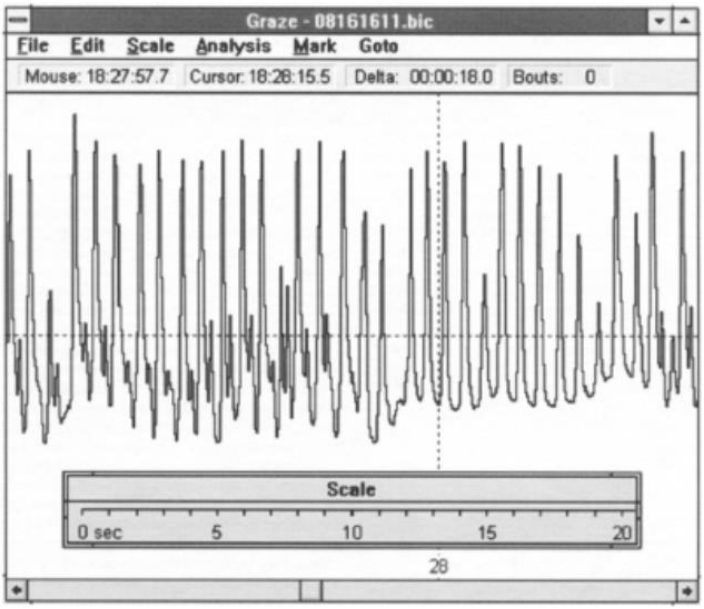

Figure 1 - The main screen of the Graze program displaying the signal referring to mandibular movements (Rutter et al., 2000).

With technological evolution, the Rumiwatch® device emerged, which is based on a pressure sensor connected to a tube with oil in conjunction with an accelerometer (Zehner et al., 2012), presenting good results in measuring ingestive behavior even in grazing environment (Werner et al., 2017). Currently, Rumiwatch® is the target of a growing number of publications that use it as a measurement tool.

Mechanical systems based on pressure sensors focus on identifying chewing movements by identifying patterns in chewing and rumination signals, being more accurate in counting rumination movements, which present a more regular pattern (Andriamasinoro et al., 2016). Despite being a particular parameter, its application is vast, as a reduction in rumination time can indicate acute stress (Herskin et al., 2004), diseases, and a general estimate of the health and well-being of groups of animals. (Paudial et al., 2018). Therefore, a detailed record of mandibular movement is essential for classification and accounting.

Rumiwatch® has a sampling rate of 10 Hz to record jaw movements and classifies them into feeding movements (in general), rumination, water intake, and non-masticatory movements. The device achieves good results in counting movements per minute. However, there is no differentiation between feeding movements such as chewing and biting (Zehner et al., 2017). These limitations in the classification of movements make it unfeasible to delve deeper into obtaining other ingestive parameters, such as consumption or quality of ingested fiber.

Considering the evolution of biosensors, which still presents some gaps, and the advancement of precision livestock farming in Brazil, the objective of this work consists of developing a data acquisition device using a pressure sensor, which enables the evaluation of mandibular movements in bovine animals. The signals obtained by the sensor are stored on a memory card for later analysis and can be sent in real-time to a computer or smartphone using Bluetooth technology.

3. Materials e Methods

3.1 System Overview

The proposed acquisition system can be better understood through the diagram shown in Figure 2. This system acquires the animal's mandibular movements through a sealed malleable tube and a pressure sensor, with the tube fixed to the bottom of a mouthpiece in direct contact with the animal's jaw. In this way, chewing movements deform the tube, generating a pressure variation translated as a differential voltage by a pressure transducer. This signal passes through an instrumentation circuit that adjusts the gain and filters the signal to be sampled by the Analog-to-Digital Converter (ADC) of a microcontroller. The algorithm embedded in the microcontroller manages the raw data, which is stored on an SD card or can be transmitted via Bluetooth for a stable operation mode.

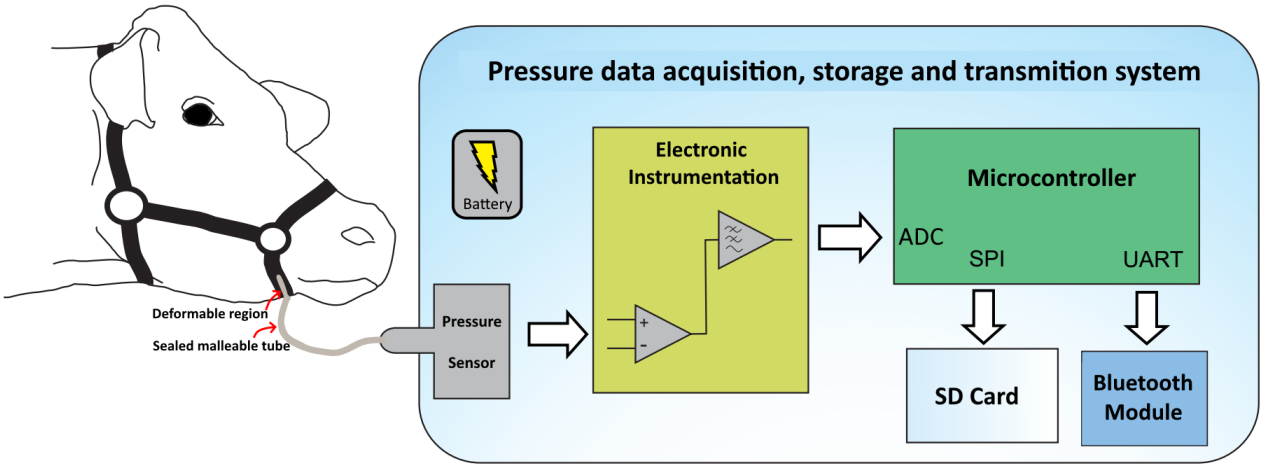

Figure 2 - Diagram of the proposed acquisition system.

The SD card was used for storage due to its high compatibility with various operating systems when using the FAT (File Allocation Table) file system, seeking easy data recovery and high system portability.

The Bluetooth 4.0 module was employed as a practical and efficient way to verify real-time data coherency, making it possible to check the status of the system to make adjustments to the sensor in the mouthpiece without proximity to the animal, as when using the LCD screen in the IGER (Rutter et al., 1997).

The following sections will explain the design methods for each stage of the mandibular movement recording system and the characteristics and configurations for each block illustrated in the diagram shown in Figure 2.

3.3 Materials

Based on the project's scope, the materials to implement the proposed system were defined and will be presented and detailed in the following subsections.

Microcontroller: The chosen microcontroller is the STM32L100RTC6 because it has the necessary resources and the availability of the 32L100CDISCOVERY development board (Figure 3), which uses this microcontroller (STMicroelectronics, 2013). This microcontroller has low power consumption characteristics, employs a 32-bit ARM Cortex M3 CPU, has 16 kB of RAM and 256 kB of Flash memory, operates with a maximum clock frequency of 32 MHz, and supports different power modes. In active mode, power consumption is around 185 uA/MHz; in low-power active

mode, consumption drops to 8.6 uA/MHz. In standby mode with RTC active, consumption is around 1.15 uA/MHz. Regarding the internal peripherals relevant to the project, we highlight the 12-bit ADC, general-purpose timers, as well as serial communication interfaces, such as SPI (Serial Peripheral Interface), I^2C (Inter-Integrated Circuit), and UART (Universal Asynchronous Receiver-Transmitter) interfaces (STMicroelectronics, 2017).

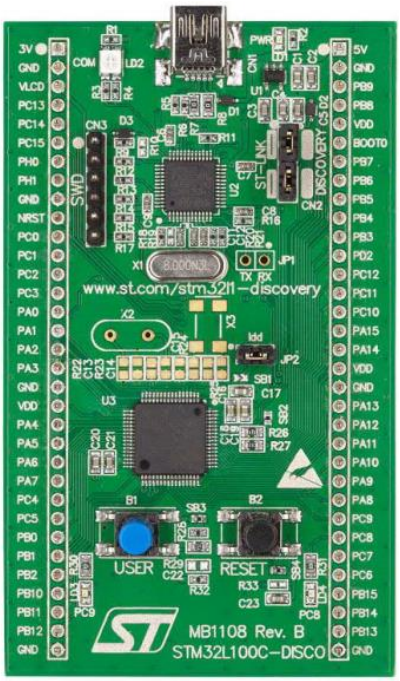

Figure 3 - Top view of 32L100CDISCOVERY board (Stmicroelectronics, 2013).

Pressure sensor: The device chosen was the MPS20N0040D-S (see Figure 4(a)), a pressure transducer (0 to 40 kPa) that converts the air pressure applied to this device into resistance. Internally, this transducer has a Wheatstone bridge (see Figure 4(b)), to which a direct voltage (e.g. 5 V) or a constant current of 1 mA can be applied. The pressure measurement range goes from 0 to 40 kPa, resulting in a voltage difference at the bridge output proportional to the pressure variation (E-Radionica, 2020).

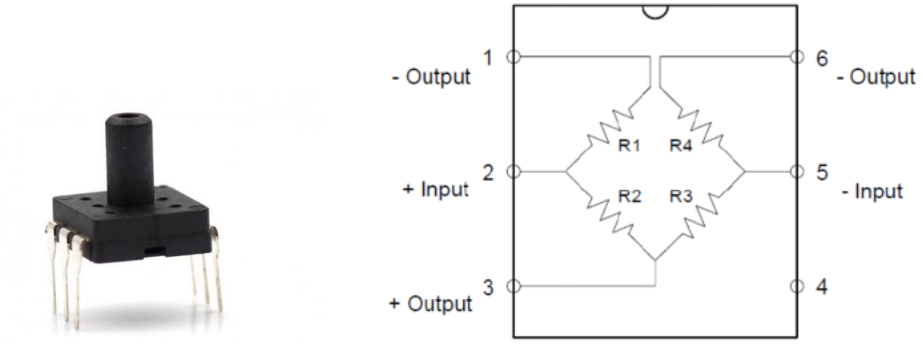

(a) (b)

Figure 4 - MPS20N0040D-S pressure transducer (E-Radionica, 2020).

Instrumentation Amplifier: The Instrumentation Amplifier (AI) applied is the INA317 device manufactured by Texas Instruments®. This instrumentation amplifier has a low power consumption profile, zero-drift, rail-to-rail output, and high precision. It features a quiescent current of 50 µV, a single power supply of 1.8 to 5.5 V, and configurable gain via an external resistor, varying from 1 to 1000 times the input differential voltage. This device offers an input with protection against EMI, reducing the effects of noise in the inputs (Texas Instruments, 2017).

Operational Amplifier (OpAmp): The OpAmp model TLV9062IDR from Texas Instruments® was chosen to implement filters. It is a low-cost OpAmp with a quiescent current of 538 µV, operating with a single power supply from 1.8 to 5.5 V, incorporating internal EMI and RFI filters at the inputs (Texas Instruments, 2018).

Battery: a Lithium Polymer (Li-Po) battery, model EHAO 404045, of 3.7 V and capable of supplying 680 mAh, was chosen due to its reduced energy capacity, reduced dimensions (94x40x45 mm), and low weight (15 g), as showm in Figure 5. This battery includes a built-in overcharge protection circuit to prevent heating if the rated charging current values are exceeded.

Figure 5 - Image of the Li-Po battery used in the proposed system.

Charge controller: The battery can be charged via a USB interface from the TP4056 device, which consists of an integrated linear charger with adjustable current and is applicable for Li-Po-type batteries. It has an internal architecture that blocks negative charging current and the possibility of reading the thermal state of the battery with a thermistor and configureble charging current capacity of up to 1000 mA (Nanjing, 2019).

Voltage regulator: To power the microcontroller and other devices, the 3 V linear regulator model TPS78230 was selected, which provides a maximum output current of 150 mA and has an ultra-low quiescent current of 1 uA. Furthermore, it has an enable pin that turns the regulator on or off (Texas Instruments, 2015).

Bluetooth module: The communication between the system and a smartphone or computer was performed through an HM-10 Bluetooth module with the CC2541 radio, as illustrated in Figure 6. This module implements the Bluetooth Low Energy (BLE) standard version 4.0 and can be supplied with a DC voltage between 2.5 and 3.3 V. Its current consumption in active mode is approximately 8.5 mA. In contrast, the current ranges from 50 to 200 uA in power-saving mode. A UART interface is provided for communication with the microcontroller, supporting a data rate of up to 115200 bps (Rajguru Electronics, 2023).

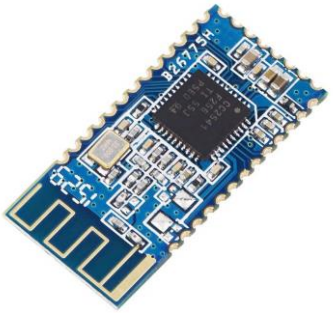

Figure 6 - Top view of the employed BLE module (Rajguru Electronics, 2023).

Mounting Box: A plastic mounting box (ABS), model CR-096 (Figure 7) and manufactured by the company Patola®, was chosen to house the acquisition system circuits, including the battery and the pressure sensor.

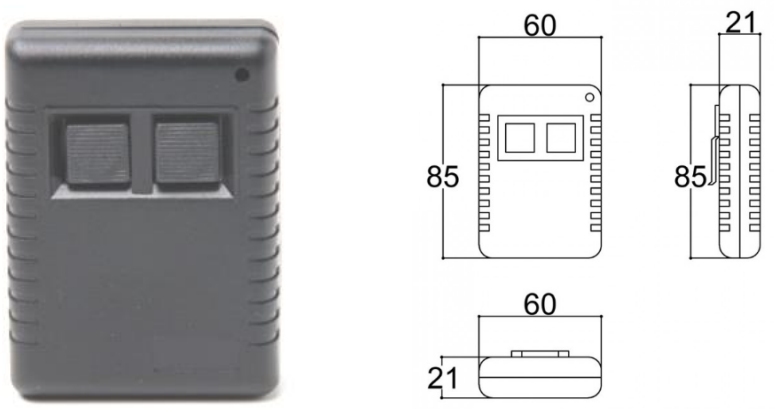

(a) (b)

Figure 7 - Mounting box model CR-096 (Patola, 2020). Measurements in mm.

Animal Halter: The halter is a type of muzzle to be attached to the animal's head. This device was made with nylon straps, metal rings, and elastic straps that adequately adjust to the animal's head. Figure 8(a) shows the mouthpiece attached to a 3D-printed life-size plastic bovine head. In the lower part of the mouthpiece, there is a housing to position the flexible tube (Figure 8(b)) in the lower part of the animal's jaw.

(a) (b)

Figure 8 - Animal halter used to fix the acquisition system.

STM32CubeIDE: This IDE allows graphical configuration of the microcontroller, code writing in C/C++ language, firmware generation, recording and debugging in the microcontroller flash memory. A Hardware Abstraction Layer (HAL) provides data structures and functions to configure and use peripherals, allowing maximum portability between the STM32 microcontrollers family (STMicroelectronics, 2024).

RTOS: The Real-Time Operating System (RTOS) used in the project was freeRTOS, with the CMSIS (Cortex Microcontroller Software Interface Standard) RTOS as an abstraction layer. This layer allows compatibility between ARM processors and other RTOS if desired. In itself, freeRTOS is a free operating system with high popularity and vast information available online (Amazon, 2017).

FatFs: is a library for implementing the FAT file system, compatible with the FAT32 standard, aimed at small embedded systems. FatFS is a free independent middleware used to implement this file system in storage media (Chen, 2020) and is available at http://elm-chan.org/fsw/ff/.

TINA-TI: is a program for developing and simulating analog electronic circuits compatible with the SPICE (Simulation Program with Integrated Circuit Emphasis) standard. In addition to being free, this program was chosen for the simulation of instrumentation circuits because the manufacturer of the amplifiers adopted provides mathematical models for simulation in TINA-TI (Texas Instruments, 2008).

Autodesk Eagle®: This EDA (Electronic Design Automation) software provided by Autodesk® allowed schematics capture and Printed Circuit Board (PCB) layout.

3.3 Methods

This section will describe the methods used in each project stage, from configuring the microcontroller to assembling the electronic circuits. Each parameter will be justified, which, for the most part, was based on preliminary tests.

Sensor and instrumentation circuit: This circuit comprises the sensor, the AI model INA317, and a fourth-order anti-aliasing filter. The differential signal from the sensors Wheatstone bridge is applied to the inputs of the INA317 device.

In practice, the appropriate gain was determined by connecting the rubber tube to the sensor and pressing the tube, simulating the deformation exerted by the animal's jaw. The voltage variation was around 10 mV. Considering the reference voltage range of 0 to 3 V adopted in the microcontroller's ADC, the gain is given by:

$$G = \frac{Vo}{Vin} = \frac{3}{0,01} = 300, \quad (1)$$

where *G* is the AI gain, *Vo* is the output voltage, and *Vin* is the voltage at the AI differential inputs. The resistance for gain adjustment in the AI was obtained from (Texas Instruments, 2017):

$$G = 1 + (\frac{100\ k\Omega}{R_G}). \quad (2)$$

In addition to the gain applied to the sensor signal, an offset was necessary to be applied to the signal due to the negative pressure in the silicone tube, which leads to an inverse differential voltage at the INA317 inputs and causes signal saturation at the output. For this, a resistive divider with a trimpot provided a DC signal entering the REF pin of the INA317, as shown in the circuit of Figure 9.

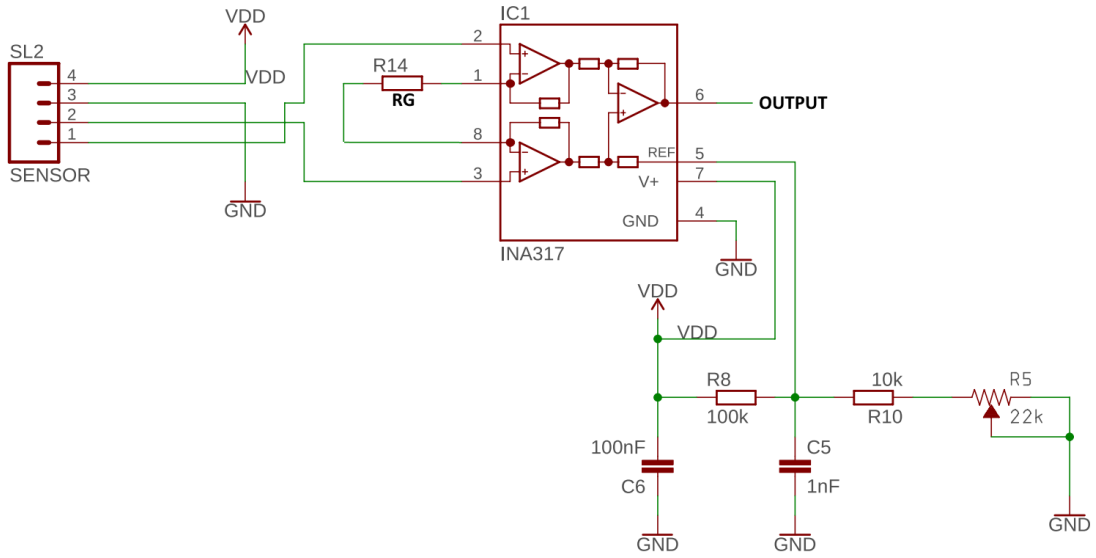

Figure 9 - Instumentation amplifier circuit.

Anti-aliasing Filter: it is a low-pass filter used in signal acquisition to avoid the phenomenon of aliasing. Although existing acquisition systems (Rumiwatch®) indicate a sampling frequency of 10 Hz, several practical tests were carried out with the pressure sensor, recording the raw values on a memory card. The recorded signals were converted from time to frequency domain using MatLab®. Some frequency components found near 15 Hz led us to assume a cut-off frequency of 15 Hz.

One of the main concerns in the filter design was the rejection of 60 Hz frequency components from the electrical power grid. With the help of the online tool known as Filter Wizard (available at: https://tools.analog.com/en/filterwizard/), it was possible to simulate different filters. The frequency response simulation of a Butterworth 4th-order low-pass filter with a 15 Hz cut-off frequency (see results section) showed that attenuations above 40 dB are evident for frequency components above 50 Hz; that is, these components represent less than 1% of the signal amplitude and can be neglected. Based on this and the sampling theorem, a sampling frequency of 100 Hz was assumed. The resulting filter circuit consists of 2 stages, each with an OpAmp, as shown in Figure 10.

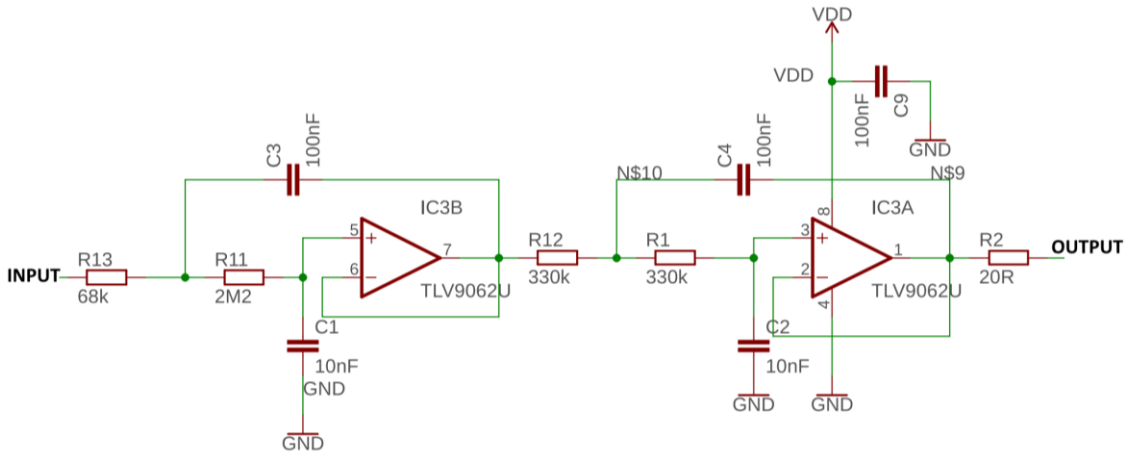

Figure 10 - Circuit of the designed Anti-aliasing filter.

Power circuit: The power circuit has a micro USB port for powering and charging the internal battery. Charging is carried out by the TP4056 device, with a charging current limit set to 300 mA, ensuring better safety and valuable life for the employed Li-Po battery. Additionally, the output supply voltages of 3 V are driven by two TPS78230 regulators, as illustrated in Figure 11. One of the regulators supplies power (Vdd) to the microcontroller, while the second regulator powers the BLE module. In this last regulator, it is possible to turn off the regulator output to further reduce energy consumption, since when turning off the BLE module via AT commands, the current drops to a range of 50 to 200 uA (datasheet HM-10), which still is significant and can drain the battery if the system is in standby state for several days. When disabling the second regulator, the current consumption drops to its quiescent current of approximately 1 uA (Texas Instruments, 2015).

Pin configuretions and initialization of microcontroller peripherals: these configuretions were carried out using the STM32CubeMX tool, which is included in the STM32CubeIDE tool. Figure 12 illustrates the microcontroller pin configuretion.

The system's user interface comprises two push buttons to set the operating mode (BT01 - turns on/off system acquisition; BT02 - turns on/off the Bluetooth data transmission) and 3 LEDs to indicate the system status (LED01 - Battery charging; LED02 - Active signal acquisition; LED03 - Active data transmission).

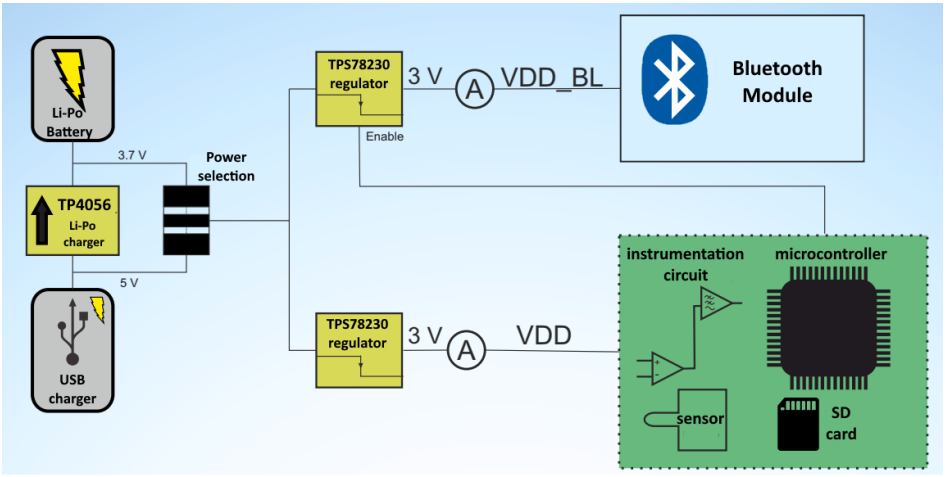

Figure 11 - Diagram of the power supply subsystem.

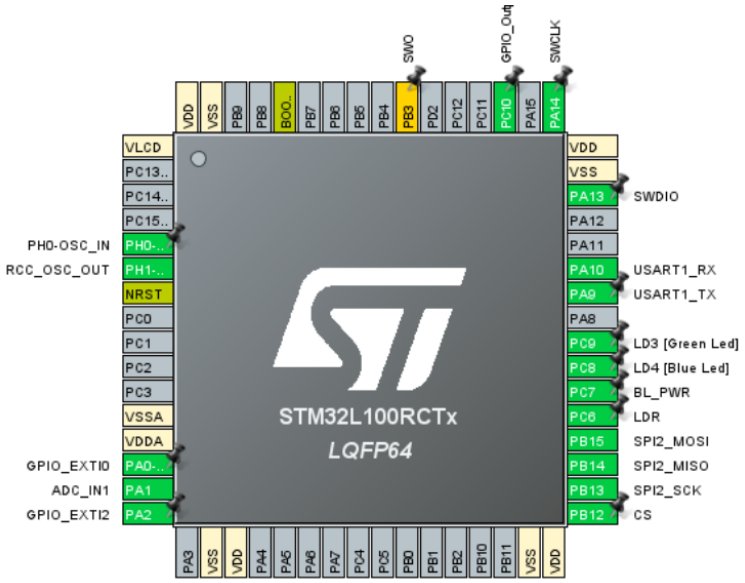

Figure 12 - Microcontroller pin configuretion through STM32CubeIDE.

Signal acquisition by the microcontroller: The anti-aliasing filter output is connected to a configured analog input pin corresponding to one of the microcontrollers ADC channels. The 12-bit ADC receives the HSI clock (16 MHz) and operates in scan mode to perform 8 consecutive conversions and store resulting data directly in a DMA (Direct Memory Access) buffer. An internal Timer 2 event triggers the ADC sampling at a frequency of 100 Hz. The DMA operates as a circular buffer. The ADC generates an interruption at the end of the 8 consecutive conversions to calculate the average of the acquired samples, which is stored in the primary buffer at the same frequency of 100 Hz.

Data recording: the averages obtained are stored in internal buffers and converted by FatFS library functions into data according to the FAT32 standard. A driver is required to communicate between the system and the SD card through an SPI interface. The development of this driver followed the code available at https://blog.domski.pl/using-fatfs-with-hal, with adaptations being made, such as the definition of new functions for SPI communication. The SPI interface was configured in full-duplex master mode with 8-bit data, allowing data to be written and read. First, the communication operates at a rate of 250 kbits/s in the SD card mounting stage, and later, the rate is increased to 4 Mbps for fast data recording.

When starting the first acquisition, a routine creates a file with the “txt” extension (E.g., “LOG0.txt”) and marks the beginning of the recording by writing “New record.” If the recording is interrupted when starting the next recording, a second file named “LOG_1.txt” is created, and so on. In an unusual operation where the system is restarted or disconnected from its power supply, it will open the last created file and update the file counter before starting a new recording, avoiding file overwrite. Finally, to read this data from the SD card on a computer, a routine developed in MatLab MatLab® reads the selected file, converts data into a 16-bit format, and presents the information in a timeline for graphical analysis.

Data transmission: the resulting data are sent to the BLE module through the UART1 interface of the microcontroller configured to 115200 bps bit rate, 8-bit data, and without parity.

Program operation: this subsection explains how the program works, including tasks and peripheral events. First, the general operation and the program flow are explained, and then each task's configuretion and semaphore are described.

The diagram in Figure 13 shows the system's operating modes and interaction with the user through BT01 and BT02. The sequence of actions in the upper state diagram with the prefix "AQ" for "ACquisition" shows the process from start to finish of data acquisition (Figure 13(a)). The sequence in Figure 13(b) shows the states with the prefix "BL" for "Bluetooth," which refers to the process from start to finish of Bluetooth transmission. The initial state of the system considers signal acquisition active and data transmission disabled (AQ_OFF and BL_OFF).

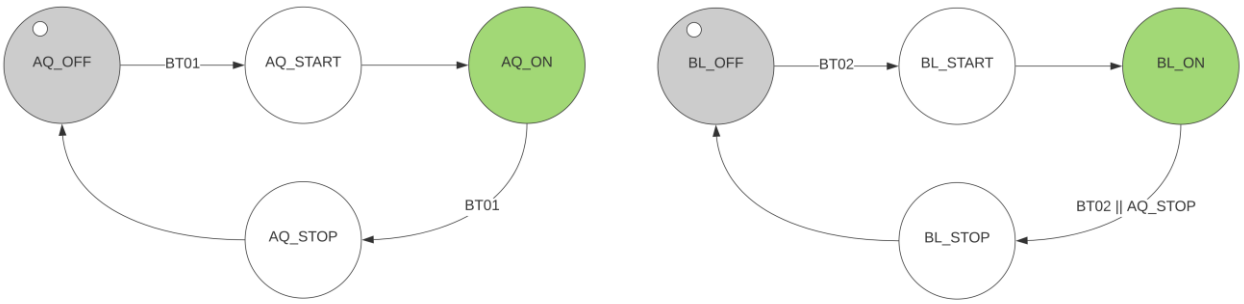

(a) (b)

Figure 13 - State diagram for the system’s operating modes.

The system starts with the acquisition turned off and enters in the energy saving mode. When pressing BT01, the system goes to the AQ_START state (Figure 13(a)), which engages SD card initialization, file system mounting, and new file creation. After this initialization, the system goes to the active AQ_ON state, where it performs the ADC conversions, calculates the average, and stores it in a buffer, which, when filled, is downloaded to the SD card. If pressing BT01 once more, the system will follow the deactivation process. In the AQ_STOP state, the ADC stops converting, and the file is closed to save the data to the SD card. Finally, the system returns to the acquisition disabled state, AQ_OFF.

Data transmittion only starts by pressing the BT02 push button if the system is in the AQ_ON state. In this case, the microcontroller activates the second regulator that powers the Bluetooth module and activates data transmission when in BL_ON state (Figure 13(b)). When pressing BT02 again or if the acquisition is interrupted (via BT01), the system goes to AQ_STOP state, suspending data transmission. Finally, the system goes to the BL_STOP state, turning the BLE module off and returning to the initial state, BL_OFF.

Tasks and interrupts in RTOS: the diagram of Figure 14 shows the detailed operation of programming with the interrupt routines and freeRTOS tasks. The system uses two tasks to execute the routine, as shown in Figure 14 (blue). “VerifyTask” is the highest priority task, which is responsible for checking the status of the buttons and performing the functions of starting and stopping the ADC acquisitions and Bluetooth data communication. The second task is “Task1”, which has lower priority and is responsible for writing data to the SD card.

The button interrupts (EXT1_interrupt) and the ADC end conversion interrupt (ADC_Interrupt) appear in red in Figure 14. EXT1_interrupt marks the timer flags and gives the semaphore to “VerifyTask,” which, with the flag marked, starts a 40 ms timer. At the end of this period, a callback function (Debouncer_timer_callback) is called, which checks the status of the button, confirms the state of the button_action state variable, and returns to “VerifyTask.”

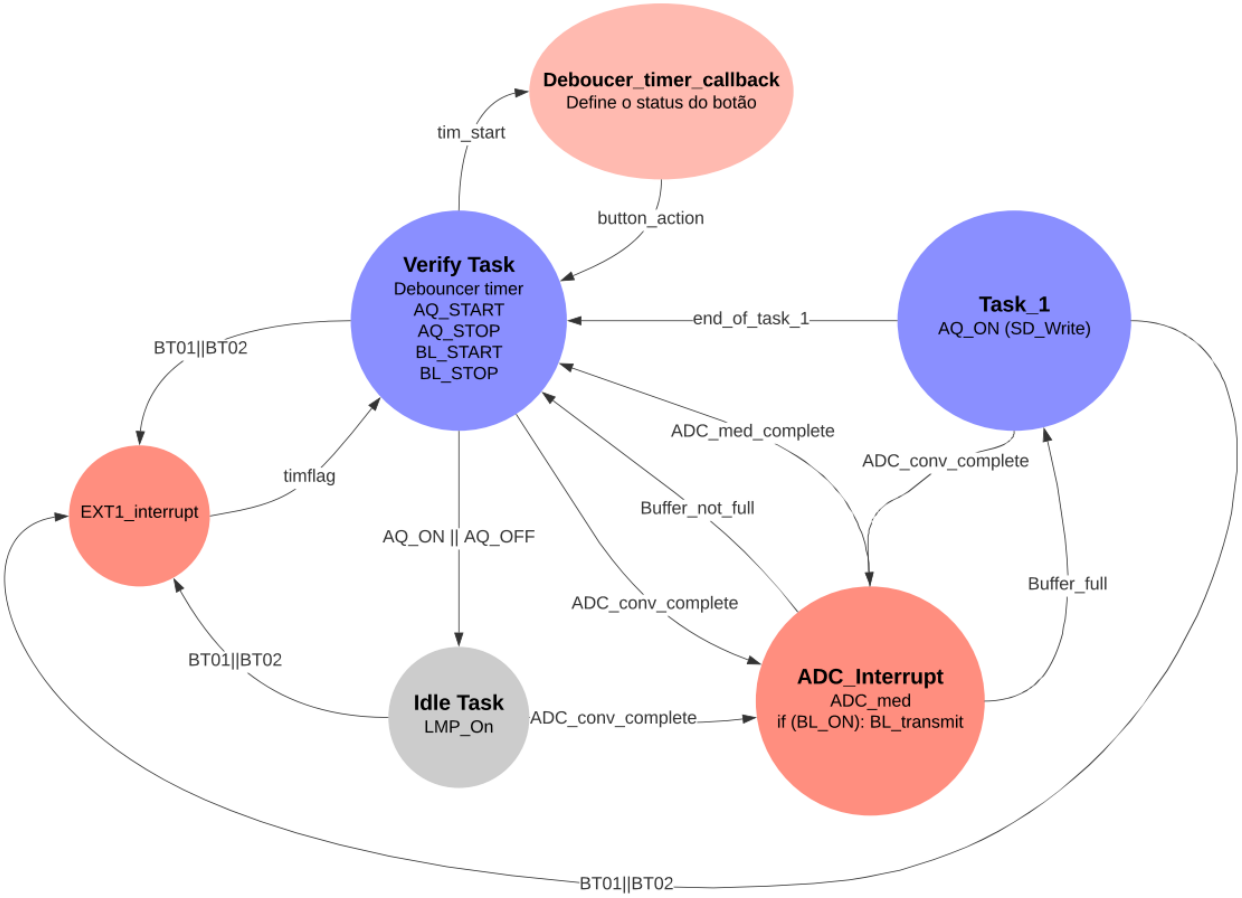

Figure 14 - Relationship between interrupt events and tasks of the RTOS.

When system acquisition is active (AQ_ON), the ADC is active, and at the end of each acquisition cycle (corresponding to a frequency of 100 Hz), the CPU enters the ADC interrupt routine (ADC_Interrupt), which calculates the average of the 8 consecutive conversions previously transferred by the DMA to the ADC buffer. A second buffer of 2048 16-bit integers stores each calculated average at a frequency of 100 Hz. During this interruption, the last computed average are transmitted if Bluetooth data communication is active (BL_ON). The average buffer fulling condition is also verified. If so, the interrupt gives the semaphore to “Task1”, which downloads the data from the average buffer to the SD card. If not, the system provides the semaphore to “VerifyTask” and, consequently, enters the “Idle Task” until the completion of the subsequent acquisition.

Marked in gray in Figure 14, Idle_task is the lowest priority system default task accessed when the system is idle. This task puts the microcontroller into power-saving mode.

Schematic Capture and PCB Layout: Both schematic capture and the PCB layout were performed using the Eagle® software. The schematic was organized into four parts: 1 - Power Subsystem (PS); 2 - Instrumentation Subsystem (IS); 3 - SD card and BLE module (SB); and 4 - STM32 Microcontroller (ST), as illustrated in Figure 15.

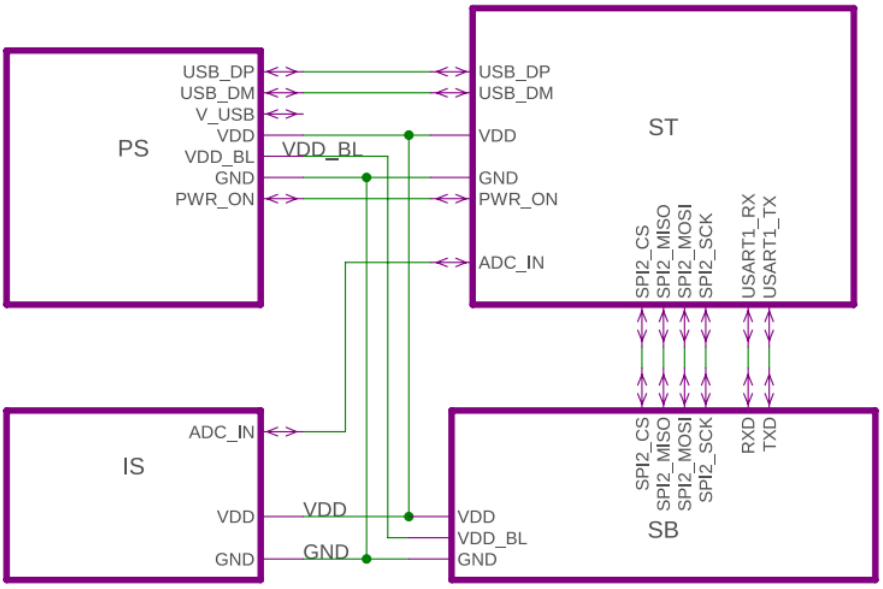

Figure 15 - Schematic organization.

The PCB layout process premises include the use a fiberglass board with two layers (top and bottom layers), the internal space of the mounting box, and the positioning of the switches, LEDs, battery, memory card socket, and SD card. Additionally, the following routing best practices were applied:

- Bring the decoupling capacitors as close as possible to the ports of their respective components;
- Avoid passing power lines (V_{dd}) under the microcontroller;
- Bring the clock crystal as close as possible to the corresponding microcontroller pins;
- Avoid straight angles (90º) on the trails;
- Maximize the GND loop throughout the circuit, but ensuring safe isolation distances to avoid short circuits when welding components.

4. Results

This section presents the results from the simulation of the anti-aliasing filter, the PCB assembly manufacturing, the PCB housing and other devices in the mounting box, the energy consumption profile, and the pressure sensor signal presented in a MatLab® graph. Due to limitations imposed by the COVID-19 pandemic from 2020 to 2022, animal experiments were not carried out.

4.1 Anti-aliasing Filter Simulation

As mentioned before, the anti-aliasing filter simulations was performed using the Analog Devices® Filter Wizard tool. Figure 16 shows the frequency response of the Butterworth 4th order low-pass filter, observing that at 60 Hz, the attenuation is almost 50 dB. This attenuation means that frequency components in the input signal above 60 Hz are attenuated more than 200 times.

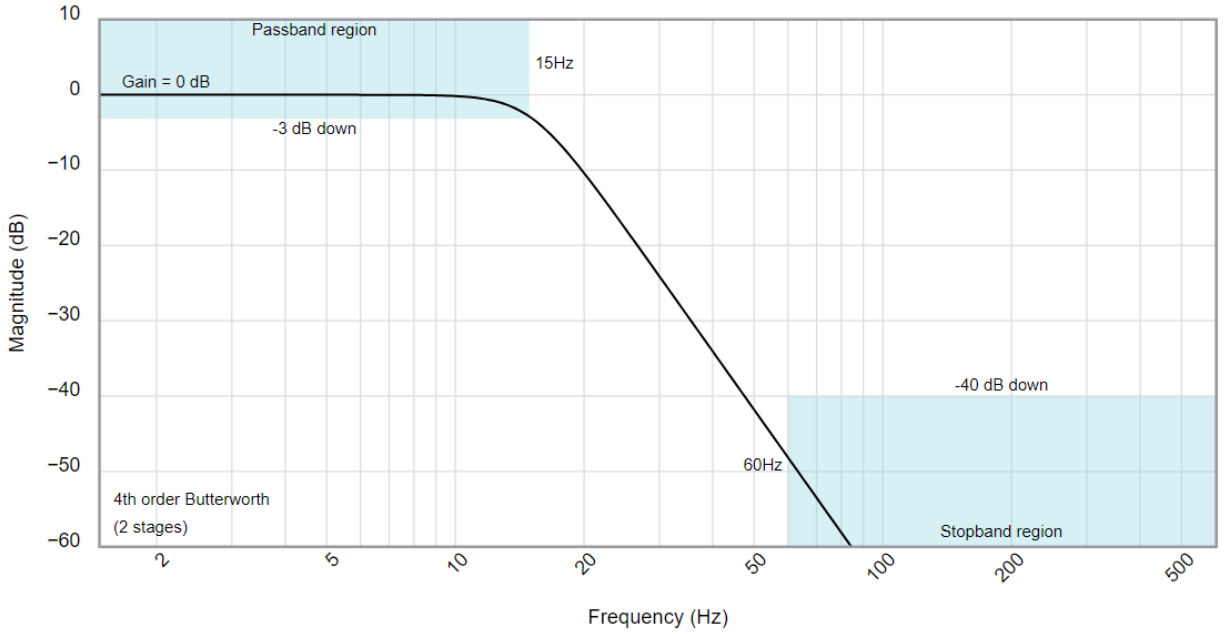

Figure 16 - Anti-aliasing designed filter response.

4.2 Printed Circuit Board

Figure 17 shows the layout created in Eagle®, with the red top layer and the blue bottom layer. Eagle® also generated the manufacturing files. With this, a double-sided FR-4 board was milled and drilled by an LPKF prototyping machine. Figure 18 shows the top layer of the resulting PCB.

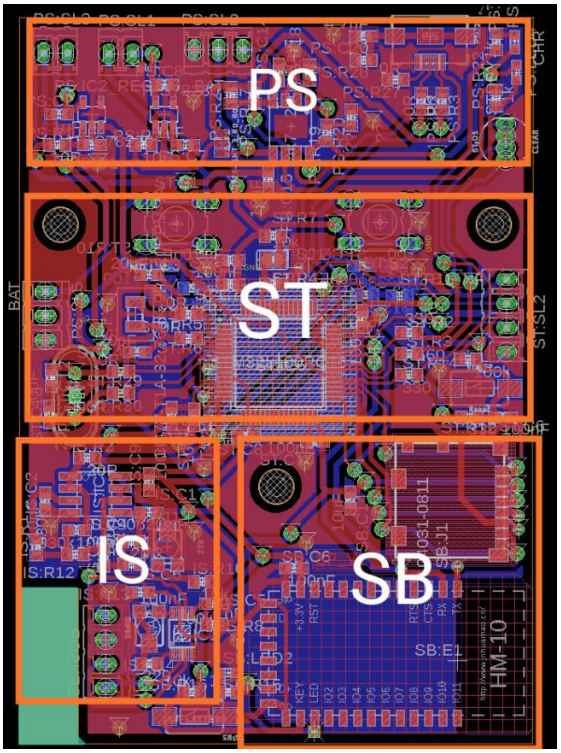

Figure 17 - Top (red) and bottom (blue) PCB layers viewed in Eagle®.

The PCB with soldered components, including an adapter board for the pressure sensor and SD card, is shown in Figure 19(a). Note that the battery was housed in the lower part of the mounting box (Figure 19(b)).

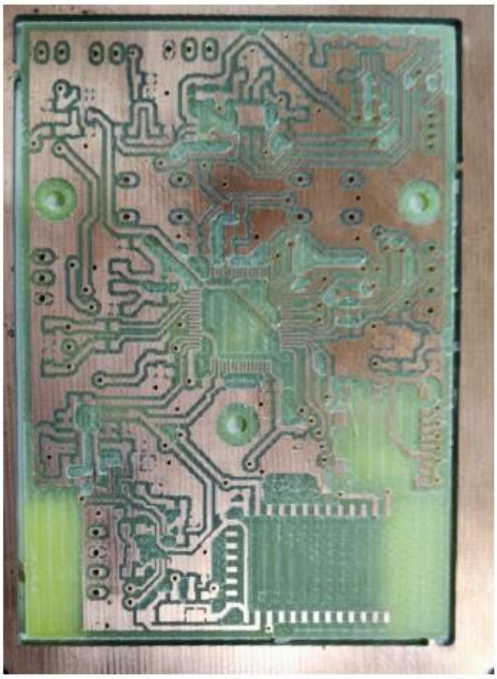

Figure 18 - Top view of machined PCB.

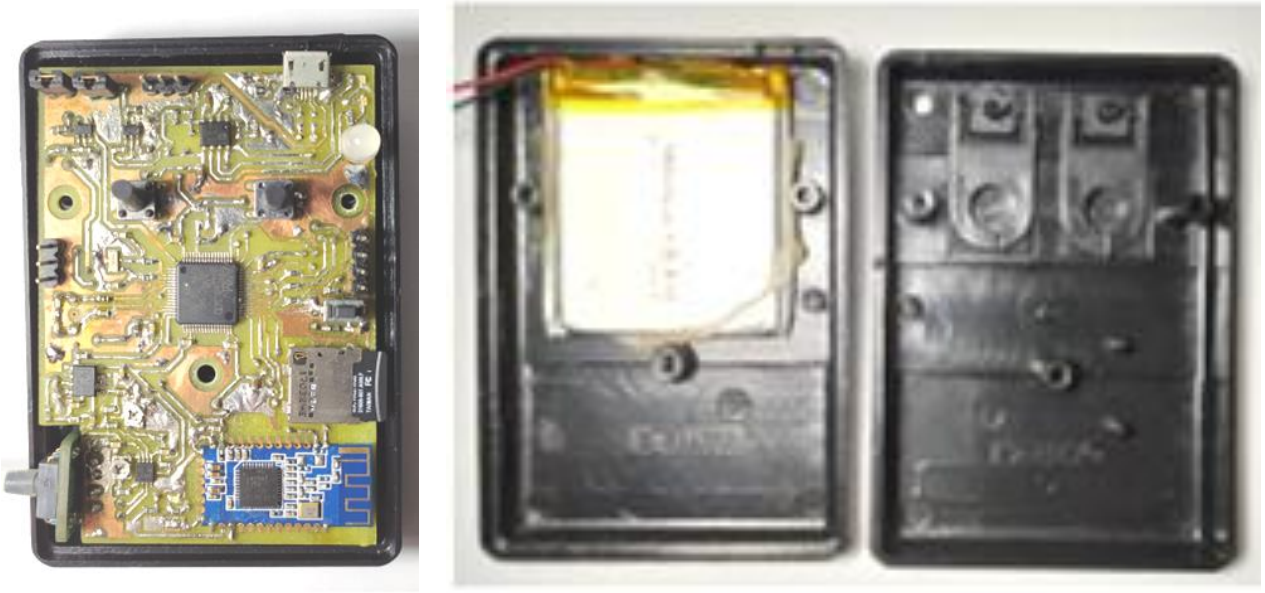

(a) (b)

Figure 19 - Housing of the populated PCB and other devices in the assembly box.

4.3 Battery autonomy assessment

The measurement of the current consumption to estimate the battery autonomy took into account the use of a Tektronix® current measurement probe model TCP0030, with a sensitivity of up to 1 mA, and a Tektronix® DPO4034 digital oscilloscope. Figure 20 shows the consumption pattern in the AQ_ON and BL_OFF states, with an average consumption of 11.6 mA with a variation of 8 to 45 mA, with peaks occurring with each recording on the SD card. The higher current consumption of the SD card endorses the importance of increasing the storage buffer to reduce the frequency of recordings.

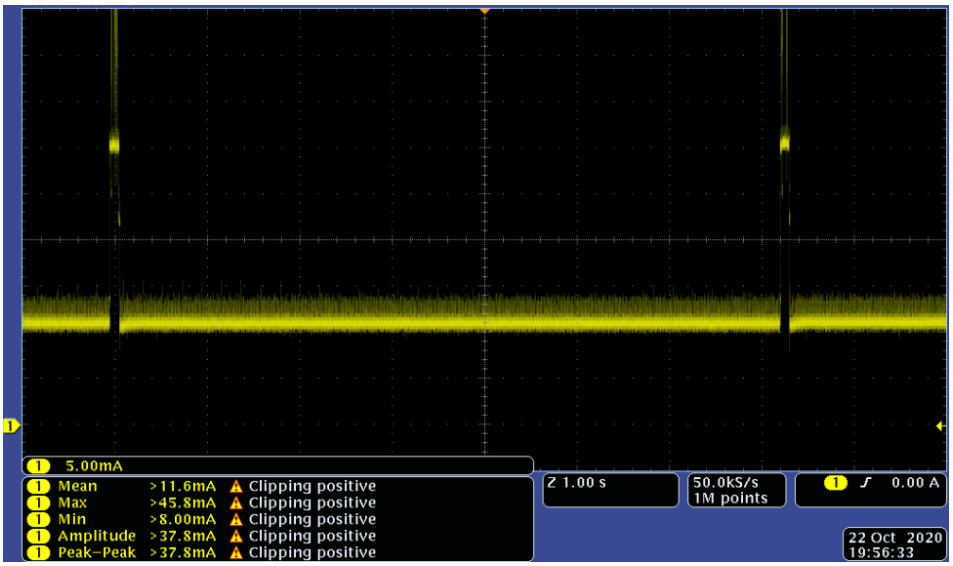

Figure 20 - System current consumption pattern in AQ_ON and BL_OFF states.

In Figure 21, it is possible to observe the consumption pattern with the Bluetooth module turned on (AQ_ON and BL_ON), observing an average consumption of 27.2 mA with peaks of almost 40 mA relating to data transmission. This 134% increase in average consumption justifies the need for the system to have an operating mode available with the Bluetooth module turned off, mainly when the noticed pressure measurement results are consistent.

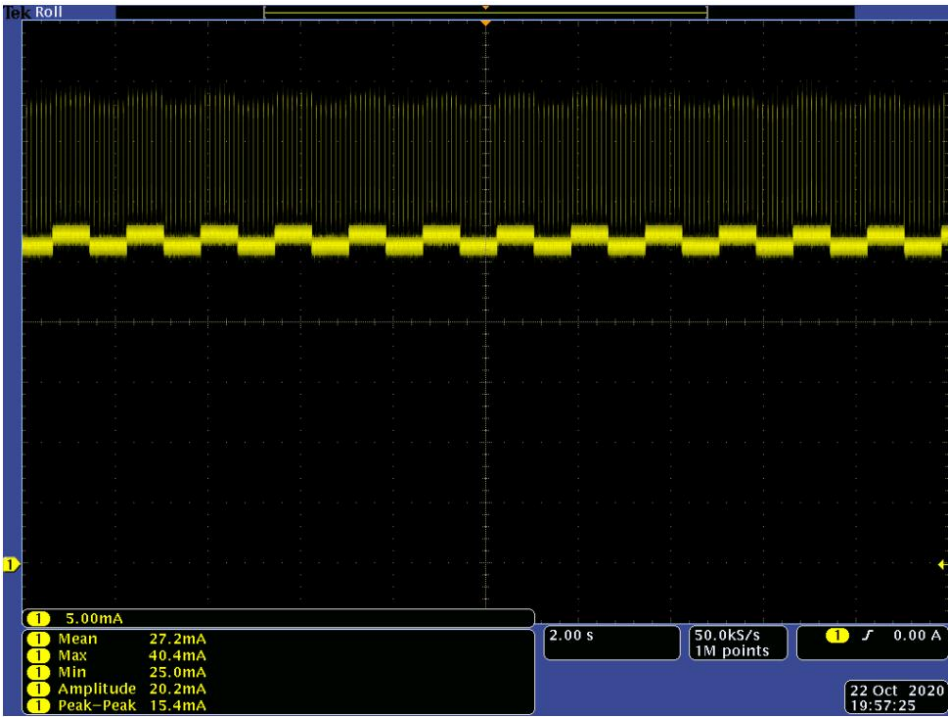

Figure 21 - System current consumption pattern in AQ_ON and BL_ON states.

It is still necessary to verify whether implementing an energy-saving mode on the microcontroller would positively affect system consumption. In Figure 22, it is possible to observe the current consumption with the energy-saving mode deactivated for the AQ_ON and BL_OFF states. The current consumption increased to 14 mA, proving that the energy-saving mode has reduced current consumption by at least 17%.

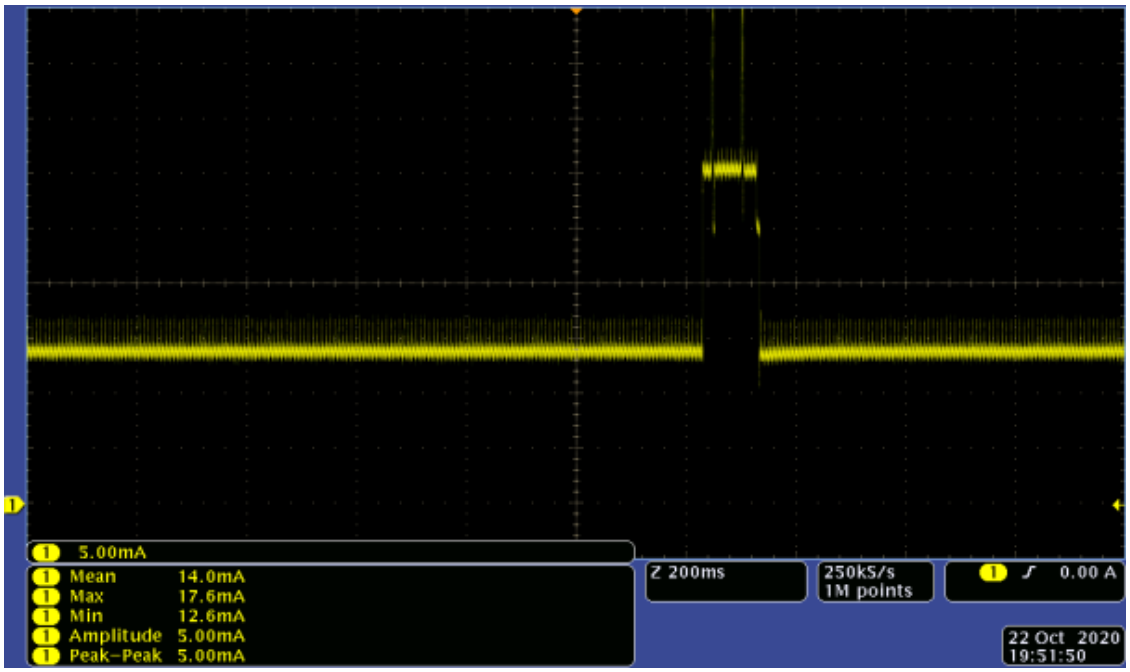

Figure 22 - Current consumption using energy-saving modes for the system in AQ_ON and BL_OFF states.

For a more accurate estimation of the system's autonomy in the primary operation phase (AQ_ON and BL_OFF), the memory card recording consumed time (T_{dr}) is approximately 100 ms based on the duration of the data recording current, which reaches the maximum current (I_{max}) consumption, as seen in Figure 22. This way, the following calculation can be made for a more accurate current average (I_{avg}), as follows:

$$I_{avg} = \frac{I_{\min} \cdot T_{ndr} + I_{\max} \cdot T_{dr}}{T_{ndr} + T_{dr}} = \\ = \frac{11.6 \cdot 7.05 + 45 \cdot 0.1}{7.05 + 0.1} = 12.24 \quad mA. \tag{3}$$

where I_{min} and T_{ndr} corresponds to the current consumption and time duration with no data recording.

Therefore, with a 680 mAh battery, it is possible to obtain an autonomy of 55 hours of continuous recording, which is superior to the IGER and ART systems but inferior to the 100 days of the Rumiwatch® (battery duration with variable sampling rate and battery capacity unknown). It is essential to highlight that this average consumption occurs with continuous recording operation at 100 Hz, which is ten times higher than the Rumiwatch® sampling rate. Another possibility for greater autonomy is to increase the battery's energy capacity, as there is space available in the mounting box to accommodate a larger battery.

4.5 Data obtained

The bench tests consisted of data acquisition and recording in a memory card, with deformations simulated by hitting the hand on the tube in three sequences with approximate intervals. Figure 23 shows the signal obtained from the average ADC results (0 to 4095) over time.

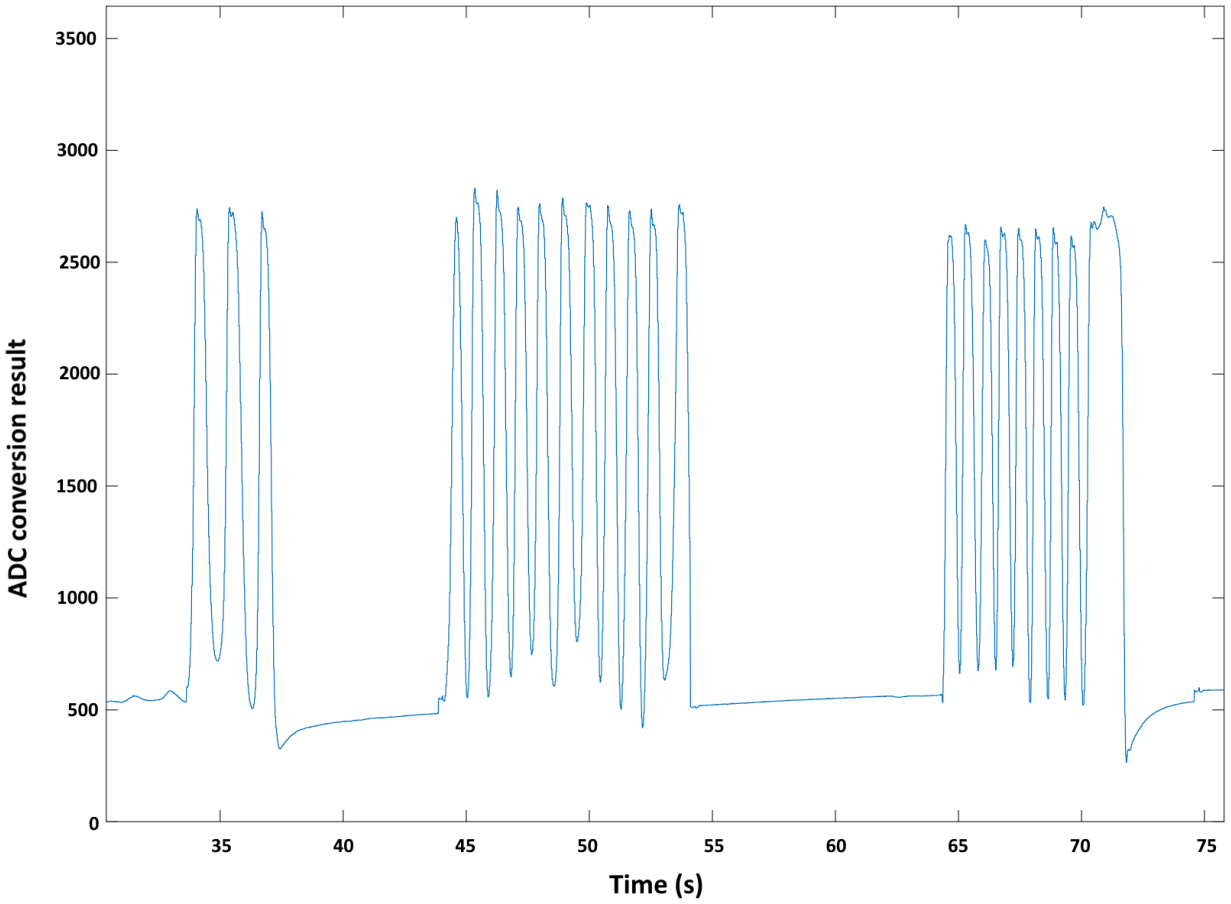

Figure 23 - Representation of the signal recorded in the memory card during the tests.

In Figure 23, it is possible to identify the moments when pressing the silicone tube by peaks in the signal. From a decision threshold applied to the signal, it is possible to detect the number of bites, which is relevant to evaluating the ingestive behavior of ruminants.

Bluetooth communication was also tested by pairing the system with a smartphone (Android operating system) and using a Serial Bluetooth Terminal application. In this application, it was possible to observe the data in real-time in text format with a simple connection, enabling a quick check of signal variations and enabling the gain adjustment of the instrumentation circuit when necessary.

5. Discussions

The literature review provided that pressure sensing is an automatic method with great potential for evaluating ruminant mandibular movements. The simplicity of the developed system allows such devices to be replicated on a large scale with the potential to spread to local research in animal behavior. By demonstrating reliability in data acquisition, the developed system can replace the current primary reference method, visual inspection. Besides that, it can serve as a reference method for evaluating other methodologies, such as surface electromyography or audio capture.

The pressure sensor's characteristic of being directly linked to mandibular movement makes this methodology an intuitive analysis, being able to detect different jaw movements of the animal, linked to ingestion or not (rumination). Adjusting the pressure tube in the mouthpiece and providing adequate gain in the instrumentation circuit was possible by viewing real-time data on a smartphone. Furthermore, due to the storage capacity of memory cards, it is possible to carry out acquisitions over long periods, revealing considerable potential for extracting attributes autonomously or in conjunction with other sensors.

The developed device had an average consumption of 12.2 mA, with an autonomy of 55 hours of data recording (680 mAh battery) at a sampling rate of 100 Hz in operating mode without data transmission via Bluetooth. Furthermore, the autonomy can be extended by recharging the battery between evaluation intervals or increasing the battery energy capacity.

The preliminary test on the bench was essential to evaluate the sealing of the tubes, as it was possible to notice that with sealing failures, over time and with an increase in the intensity and frequency of applied compressions, air leaks occur. This leakage causes a decrease in signal amplitude and a shift in the signal offset due to the emergence of negative pressure in the tube. Regarding the aspect of the signal shown in Figure 23, when compared with the IGER signal shown in Figure 1, a significant similarity is observed between these signals. This comparison allows preliminary validation of the response of the developed system.

6. Conclusion

This work presented the development of an electronic system for acquiring, storing, and transmitting signals from a pressure transducer to monitor the ingestive behavior of ruminants. The system installed on a full-size prototype bovine head allowed preliminary bench tests. Compression movements were applied to a sealed silicone tube filled with air, causing pressure variations detected by a pressure transducer. After amplifying and filtering the transducer signal, it was acquired at a sampling frequency of 100 Hz. By transmitting the data to a smartphone via Bluetooth, it was possible to check the signal, adjust the gain of the instrumentation amplifier, and find the best positioning of the silicone tube in the mouthpiece. By reading the data recorded on a memory card, it was possible to obtain the signal profile, graphically demonstrating the expected functioning of this type of sensor. We expect this work will expand the study of the ingestive behavior of ruminants, making it possible to improve management techniques and, consequently, contribute to the evolution of precision livestock farming in Brazil.

Acknowledgements

The authors appreciate the financial support from: Coordenação de Aperfeiçoamento de Pessoal de Nível Superior - Brasil (CAPES), Conselho Nacional de Desenvolvimento Científico e Tecnológico (CNPq), Fundação Araucária (FA), Financiadora de Estudos e Projetos (FINEP), Universidade Tecnológica Federal do Paraná - UTFPR, and Instituto de Desenvolvimento Regional do Paraná (IDR-PR).

References

Andriamasinoro, A. L. A., Bindelle, J., Mercatoris, B., Lebeau, F. (2016) A review on the use of sensors to monitor cattle jaw movements and behavior when grazing. *Biotechnol. Agron. Soc. Environ.*, 20(1), 273–286. doi: https://doi.org/10.25518/1780-4507.13058

Amazon Web Services. (2017). The FreeRTOS™ Reference Manual. Manual. Disponível em: https://www.freertos.org/fr-content-src/uploads/2018/07/FreeRTOS_Reference_Manual_V10.0.0.pdf

Beauchemin, A., Zelin, S., Genner, D., Buchanan-Smith, J.G. (1989). An Automatic System for Quantification of Eating and Ruminating Activities of Dairy Cattle Housed in Stalls. *Journal of Dairy Science*, 72(10), 2746-2759. doi: https://doi.org/10.3168/jds.S0022-0302(89)79418-2

Berckmans, D. (2008). Precision livestock farming (PLF). *Computers and Electronics in Agriculture*, 62(1), 1. doi: https://doi.org/10.1016/j.compag.2007.09.002

Berckmans, D. (2017). General introduction to precision livestock farming. *Animal Frontiers*, 7(1), 6–11. doi: https://doi.org/10.2527/af.2017.0102

Chen, Z. (2020). Design and implementation of FATFS data exchange with multiple storage media based on single-chip microcomputer. *Journal of Physics: Conference Series*, 1550(3), 1-4. doi: https://doi.org/10.1088/1742-6596/1550/3/032090

E-Radionica. (2020). Pressure Sensor MPS20N0040D-S. Manual, 3–5. Available at: https://e-radionica.com/en/air-pressure-sensor-mps20n0040d-d.html

Herskin, M.S., Munksgaard, L., Ladewig, J. (2004). Effects of acute stressors on nociception, adrenocortical responses and behavior of dairy cows. *Physiol. Behav.*, 83(3), 411-20. doi: https://doi.org/10.1016/j.physbeh.2004.08.027

Law, S. E ., Sudweeks, E. M. (1975). Electronic Transducer for Rumination Research. *Journal of Animal Science*, 41, 213–218.

NanJing Top Power ASIC Corp. (2019). TP4056 1A Standalone Linear Li-lon Battery Charger with Thermal Regulation in SOP-8. *Datasheet*, 1-3.

Neethirajan, S., Tuteja, S. K., Huang, S., Kelton, D. (2017). Recent advancement in biosensors technology for animal and livestock health management. *Biosensors and Bioelectronics*, 98(1), 398–407. doi: https://doi.org/10.1016/j.bios.2017.07.015

Norton, T., Berckmans, D. (2018). Engineering advances in Precision Livestock Farming. *Biosystems Engineering*, 173(1), 1–3. doi: https://doi.org/10.1016/j.biosystemseng.2018.09.008

Nydegger F., Gygax L., Egli, W. (2011). Mesure automatique des mouvements de rumination par capteur de pression. *Recherche Agronomique Suisse*, 2(2), 60-65.

OECD/FAO. (2021). OECD-FAO Agricultural Outlook 2021-2030. *OECD Publishing.* doi: https://doi.org/10.1787/19428846-en.

Patola Eletroplasticos. (2020). Catálogo Digital de Produtos. Disponível em: https://www.patola.com.br/pt_PATOLA_CATALOGO_DIGITAL.pdf

Paudyal, S., Maunsell, F. P., Richeson, J. T., Risco, C. A., Donovan, D. A., Pinedo, P. J. Rumination time and monitoring of health disorders during early lactation. (2018). *Animal*, 12(7), 1484-1492. doi: https://doi.org/10.1017/s1751731117002932

Penning, P. D. (1983). A technique to record automatically some aspects of grazing and ruminating behaviour in sheep. *Grass and Forage Science*, 38(2), 89–96.

Rajguru Electronics. (2023). HM 10 TTL BLE Bluetooth Module. Datasheet. Disponível em: https://www.rajguruelectronics.com/ProductView?tokDatRef=MjI5OA==&tokenId=NDA=&product=HM-10%20TTL%20Original%20Module#datasheet

Ribas, M. N., Cavalcanti, L. F. L., Machado, F. S., Paiva, C. A. V., Pereira, L. G. R. (2017). Pecuária de precisão: uso de tecnologias para apoio à tomada de decisão. In: *Congresso Brasileiro De Zootecnia*, 27.

Rutter, S. M., Champion, R. A. and Penning, P. D. (1997). An automatic system to record foraging behaviour in free-ranging ruminants. *Applied Animal Behaviour Science*, 54(2-3), 185-195. doi: https://doi.org/10.1016/s0168-1591(96)01191-4

Rutter S. M. (2000). Graze: a program to analyze recordings of the jaw movements of ruminants. *Behav Res Methods Instrum Comput.*, 32(1), 86-92. doi: https://doi.org/10.3758/bf03200791

Schofield, C. P., Mottram, T. T., Beaulah, S. A., Wathes, C. M., Lines, J. A., Frost, A. R. (2002). A review of livestock monitoring and the need for integrated systems. *Computers and Electronics in Agriculture*, 17(2), 139–159. doi: https://doi.org/10.1016/S0168-1699(96)01301-4

STMicroelectronics. (2013). 32L100CDISCOVERY discovery kit for STM32L100 Value Line microcontrollers, User manual, 1–30. Retrieved from: https://www.st.com/resource/en/user_manual/um1656-32l100cdiscovery-discovery-kit-for-stm32l100-value-line-microcontrollers-stmicroelectronics.pdf

STMicroelectronics. (2017). Ultra-low-power 32b MCU ARM®-based Cortex®-M3, 256KB Flash, 16 kB SRAM, 4 kB EEPROM, LCD, USB, ADC, DAC, memory I/F. Datasheet. Retrieved from: https://www.st.com/resource/en/datasheet/stm32l100rc.pdf

STMicroelectronics. (2024). STM32CubeIDE user guide. Manual. Retrieved from: https://www.st.com/resource/en/user_manual/um2609-stm32cubeide-user-guide-stmicroelectronics.pdf

Texas Instruments. (2008). GettingStartedwithTINA-TI™. Quick Start Guide. Retrieved from: https://www.ti.com/lit/pdf/SBOU052A

Texas Instruments. (2015). TPS782 500-nA IQ,150-mA, Ultra-Low Quiescent Current Low-Dropout Linear Regulator. Datasheet. Retrieved from: https://www.ti.com/lit/gpn/tps782

Texas Instruments. (2017). INA317 INA317 Micro-Power (50-µA), Zero-Drift, Rail-to-Rail-Out Instrumentation Amplifier. Datasheet. Retrieved from: http://www.ti.com/lit/ds/symlink/ina317.pdf

Texas Instruments. (2018). TLV900x Low-Power , Rail-to-Rail In and Out, 1-MHz Operational Amplifier. Retrieved from: https://www.ti.com/lit/ds/symlink/tlv9001.pdf

United Nations, Department of Economic and Social Affairs, Population Division of. (2022). World Population Prospects 2022: Summary of Results. UN DESA/POP/2022/TR/NO (3).

Werner, J., Leso, L., Umstatter, C., Niederhauser, J., Kennedy, E., Geoghegan, A., Shalloo, L., Schick, M., O'Brien, B. (2018). Evaluation of the RumiWatchSystem for measuring grazing behaviour of cows. Journal of Neuroscience Methods, 300(1), 138-146. doi: https://doi.org/10.1016/j.jneumeth.2017.08.022

Zehner, N., Niederhauser, J., Nydegger, F., Grothmann, A., Keller, M., Hoch, M., Haeussermann, A., Schick, M. (2012). Validation of a new health monitoring system (RumiWatch) for combined automatic measurement of rumination, feed intake, water intake and locomotion in dairy cows. In: International Conference of Agricultural Engineering CIGR. Valencia, Spain.

Zehner, N., Umstätter, C., Niederhauser, J. J., Schick, M. (2017) System specification and validation of a noseband pressure sensor for measurement of ruminating and eating behavior in stable-fed cows. *Computers and Electronics in Agriculture*, 136(1), 31-41. doi: https://doi.org/10.1016/j.compag.2017.02.021